Experimental Investigation of the Tribological Performance and Statistical Analysis of WC-Co-10%TiC Cermet

UDC:620.178.16:669.018.25
Original scientific paper https://doi.org/10.46793/aeletters.2026.11.1.3

Riad Harouz[1*], Djamel Zelmatı [2,3]

[1]Electromechanical and Operational Safety Laboratory, Department of Mechanical Engineering, Faculty of Science and Technology, Mohamed Chérif Messaadia University, Souk-ahras, Algeria
[2]Research Center in Industrial Technologies (CRTI), P.O. Box 64, Cheraga, Algiers, 16014, Algeria
[3]LRTAPM, Research Laboratory of Advanced Technology in Mechanical Production, Department of Mechanical Engineering, Faculty of Engineering Science, Badji Mokhtar - Annaba University, BP 12, 23000, Annaba, Algeria

Abstract:
This study investigates the tribological performance of a WC–Co cermet reinforced with 10% TiC under severe tribological conditions. Disc tribometer tests (cermet) against an Al_2O_3 ball were conducted at 650°C, 0.5 m/s sliding speed, 20 N load, and a sliding distance of 5000 m. Besides, a statistical analysis of the friction coefficient. The results reveal a stable coefficient of friction of μ=0.43, indicating excellent thermal and tribological stability. The analysis demonstrates that the friction coefficient follows a logistic distribution with lower dispersion and weaker parameter correlation compared to the normal distribution. SEM/EDS analyses show the formation of a dense, continuous tungsten-rich oxidized tribofilm, enhancing wear resistance and surface protection, and increasing cermet durability.

ARTICLE HISTORY
Received: 3 October 2025
Revised: 14 January 2026
Accepted: 12 February 2026
Published: 31 March 2026

KEYWORDS
Cermet WC-Co-10%TiC, Pin-on-disc, Friction, wear rate, Microstructural analysis, Statistical analysis

1. INTRODUCTION

The cermet WC-Co is used in several industrial applications involving dry contact under severe tribological parameters**,** among equipment components such as drilling tools, machining cutting tools, hot-rolling dies, and aeronautical equipment [1–4]. Many applications involve dry sliding conditions between interacting surfaces in relative motion, where wear is the primary failure mode. Furthermore, many researchers have studied how the normal contact load, sliding speed, temperature, lubrication, and contact surface geometry influence the tribological performance of WC-Co cermets [5–10]. Devices and equipment made of WC-Co cermet, such as hot-rolling dies, begin to oxidize during hot deformation when the contact surface temperature reaches approximately 600°C [11]. As a result, friction and wear intensify, leading to accelerated material degradation and reduced device durability [12]. The addition of a low percentage of titanium carbide (TiC) to the tungsten carbides (WC-Co) is regarded as a recent method for enhancing the tribological behavior of these materials. TiC, as a reinforcing particle, is intended for applications where good wear resistance and high hardness are major requirements [13–17]. TiC is a ceramic material known for its high-temperature properties and thermal stability, owing to its high melting point (3065°C), hardness, and exceptional wear resistance under severe tribological conditions [18]. Furthermore, they offer good corrosion and oxidation resistance, and a relatively low density [19]. Also, TiC has excellent physical and chemical properties, including high hardness, a high melting point, low density, and good thermal stability. Similarly, TiC is widely used as a reinforcing phase in metal matrix composites [20–23]. Recently, it has been proven that tribological characteristics can be improved by

*CONTACT: Riad Harouz, e-mail: r.harouz@univ-soukahras.dz

adding a percentage of TiC to WC-Co cermet [24–27]. The sliding wear resistance of these cermets is influenced by their microstructural characteristics, such as shape, structure, size, and, in particular, the distribution of hard particles [28–30]. However, no work has been reported to date on the tribological dry sliding behavior of WC-CO-10% TiC cermet under (Temperature 650°C, sliding speed 0.5 m/s, normal load 20 N, and sliding distance 5000 m). The aim of this research was to study the tribological behavior of friction and wear and to perform a statistical analysis of cermet.

This statistical analysis was conducted to ensure the reliability and reproducibility of the tribological results. Several wear tests were carried out under identical experimental conditions, and the mean values of the coefficient of friction and the wear rate were calculated. Data dispersion was assessed using standard deviation and variance. Furthermore, a regression analysis was used to evaluate the relationship between the sliding distance and the coefficient of friction. The results demonstrate a strong correlation during the break-in phase, followed by a plateau corresponding to steady state. This statistical approach validates the experimental trends and strengthens confidence in the tribological performance of the developed WC-Co-10TiC cermet [30–33].

In this study, a WC-Co-10%TiC cermet was synthesized and tested under dry friction conditions to evaluate the evolution of the friction coefficient and wear rate. A methodology was developed to quantify volumetric wear and wear rate from four-section profile measurements of the worn track. The results demonstrate that cermet exhibits exceptionally low wear rates under dry friction loading, which is corroborated by its high microstructural stability. SEM/EDS analyses were performed to identify and characterize the wear mechanisms governing its tribological behavior. Furthermore, a statistical analysis of the coefficient of friction data was conducted using probability density functions and cumulative distribution functions. The results indicate that extreme value distributions accurately describe the behavior of the coefficient of friction, thus providing a robust framework for its statistical characterization

2. MATERIAL AND METHODS

In the present work, cermets composed of WC, Co, and 10% TiC powders were manufactured using conventional powder metallurgy techniques and liquid-phase sintering. These cermets were then used to study the tribological behavior under dry sliding wear parameters. Hardness Testing Instruments Machine (Induno Olona, Varese, Italy) was used to measure the average hardness and density of the developed material, and the sample densities were determined using the Archimedes method. In a high-temperature tribometer (pin-on-disk), the cermet samples were tested between a WC-Co-10%TiC disk and an alumina ball (Al_2O_3). The alumina has good resistance properties to wear and mechanical strength at high temperatures, intended for cermet friction tests [29,34]. The experimental work was carried out using friction tests to measure the friction coefficient. A 3D surface profilometer was used to determine the track wear rates (optical microscope Contour GT-I Bruker Nano Surfaces Division, Tucson, AZ, USA). The profilometer instrument is driven by Vision software to assess the wear track image. Besides, this research work studies wear through friction tests under parameters: sliding speed (0.5 m/s), temperature (650°C), and a long distance (5000 m), estimated to correspond to a sliding time (2 hours and 46 minutes) to analyze the degradation of the microstructure of the worn track. The choice of the temperature and sliding speed test parameters is justified by their occurrence in the hot-rolling and crushing processes in which the studied cermets are used. Also, a long distance (5000 m) is needed in order to obtain a worn volume for this type of material (cermet), which has high hardness, to allow microstructural analysis. The impact of temperature, speed, and sliding distance on the tribological behavior, friction coefficient, and wear rate was investigated. The results include a comparison between the experimental results through the worn track, using the Archard model, for both wear volume and wear rate. The data analysis suggests that the friction coefficient remains stable. The addition of 10% TiC improved the wear resistance, friction behavior, and overall tribological properties of the material compared with previous work by Harouz et al. [3,21]. A microstructural SEM/EDS analysis of the worn track material was conducted to examine the degradation mechanisms. Besides, the micrograph analysis revealed that the wear mechanism was predominantly adhesive, with the presence of an oxidized layer generated on the wear track. This exhibited a perfect stability of the friction coefficient under these conditions.

The aim of this research on the tribological performance and statistical analysis of the WC-Co-10%TiC cermet is to develop the following steps:

- Measure the wear volume after the friction test of the worn track of the cermet sample using a theoretical method based on the track cross-section profile in order to estimate the lifetime of the cermet sample.
- A statistical analysis of the tribological parameters, the coefficient of friction responsible for estimating the lifetime of the cermet, and also a statistical analysis of the density, while exploiting experimental data.

2.1. Experimental Details

The experimental procedure for preparing the samples (cermets) was carried out at laboratory 05025, Batna, Algeria. The tests and analyses of the samples were conducted at the Laboratory of Metallic Materials Science, ULg-MMS, Belgium.

2.1.1. Cermet Sample Preparation Procedure

Powder Preparation: The first step is to grind the raw powders (WC, Co, and TiC) in a ball mill. The powders are weighed according to their mass fraction to ensure a homogeneous mixture. The grinding process is carried out in a humid environment, using ethanol (C_2H_5OH) as the grinding medium, for an average of 24 hours. This is followed by a drying operation in a stirred oven to evaporate the ethanol, generally for 30 to 40 minutes. The dried powder is then mixed with an organic binder to promote particle agglomeration. Finally, the agglomerated powder is sieved under forced pressure to remove oversized particles and achieve a homogeneous particle size distribution.

Compaction: The sieved powder was compacted using a hydraulic press. The compaction parameters were selected based on the sample's density and geometry. The sample dimensions (15 mm thick × 35 mm in diameter) were designed to compensate for post-sintering shrinkage. An average compaction pressure of 15 MPa was applied, followed by oven drying for 3 to 4 hours to ensure complete volatilization of the binder.

Sintering: Total cycle duration averages 10 hours using a standardized sequence:

- Heating to 600°C,
- Ramping to 1430°C,
- Controlled cooling.

This process fuses powder grains through solid-state diffusion. Sintering occurs in a tubular furnace chamber under a protective argon atmosphere. Prior to sintering, the furnace is purged with a non-oxidizing Ar/H_2 gas mixture. Fig.1 illustrates the Cermet Sample Preparation Procedure.

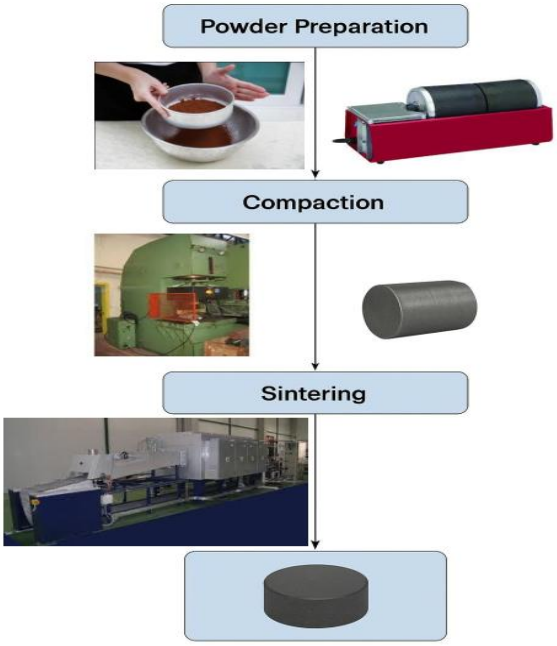

Fig.1. Cermet samples preparation procedure [3,21]

The WC-Co-10%TiC sample used in this study was produced by conventional powder metallurgy techniques. The powders are manufactured and commercialized by the Norinco Group of China. After weighing, the powders were mixed in a ball mill for 24 h with the addition of methanol (C_2H_5OH). The mixture was then dried in an electric furnace (YZM-40, China) for 30 minutes at a temperature of 70°C. The particle sizes and densities of the WC, Co, and TiC powders are listed in Table 1.

Table 1. Size particles and powders density

Powders	Size (µm)	Density (g/cm^3)
WC	0.1	7.5
Co	1	8.9
TiC	2	8

A Hardness Testing Instrument (Induno Olona, Varese, Italy) was used to measure the average hardness and density of the developed material, and the sample densities were determined using the Archimedes method. The measured density and hardness of the samples, as given in Table 2, are practically consistent with ISO compositions.

Table 2. Typical density and hardness of the elaborated material

Sample	Density (g/cm^3)	Hardness HRC (MPa)
WC-Co-10%TiC	11.74	74.4

The alumina ball (Al_2O_3) used for the friction tests has a diameter of 6 mm, with its density and hardness values reported in Table 3. To avoid premature adhesive wear on the ball, the surface in direct contact with the sample was slightly modified after each step of the friction test.

Table 3. Density and hardness properties of an alumina Al_2O_3 ball

	Density (g/cm^3)	Hardness HV (MPa)
Ball properties	3.2	1800

2.1.2. Friction Test

The developed sample (WC-Co-10%TiC) was subjected to rotational sliding wear tests on a pin-on-disc tribometer (CSM Instruments, Switzerland). The applied normal force was set to 20 N, with a linear speed of 500 mm/s and a contact temperature of 650°C between the ball and the sample (cermet), over a sliding distance of 5000 m (2h 46min), as mentioned in Table 4.

Table 4. Parameters of applied wear tests

Load P (N)	Sliding speed V (m/s)	Temperature T (°C)	Distance D (m)
20	0.5	650	5000

To simulate the environment of a hot-rolling deformation tool, a dry sliding test was conducted. During the experimental test, it is noteworthy that the first wear track formed after 2 hours and 46 minutes of sliding distance. The pin-on-disc test measures sliding distance over time, and the resulting properties include the friction coefficient, friction force, sample temperature, oven temperature, and depth of penetration [3,26].

2.1.3. The Experimental Procedure for Measuring the Wear Track Volume

A wear track was formed following the friction test of the material on the tribometer, as shown in Fig. 1, and Fig. 2a shows the four measurement points on the worn track Fig.2. The sample dimensions are a disc of diameter 32 mm and thickness 15 mm. Using a profilometer and a two-dimensional optical microscope, this wear track was analyzed in Fig. 2b.

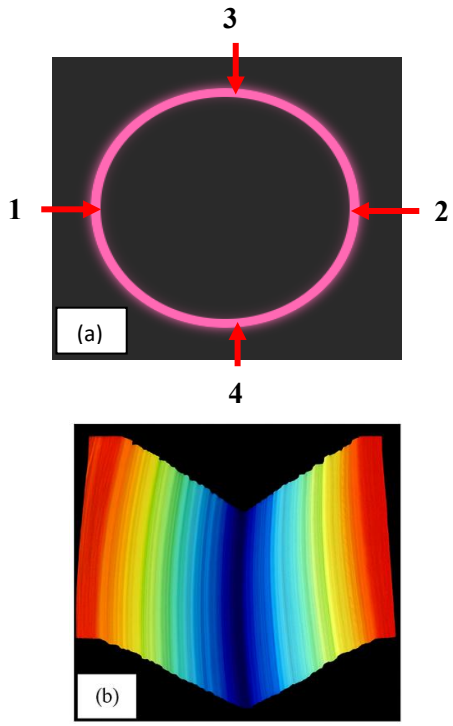

Fig. 2. Vision image of a section of the wear track: (a) The four measurement points on the wear, and (b) Profile of the geometry of the wear track

This testing procedure is crucial in determining the resistance of the developed material to sliding wear. A 3D surface profilometer was used to determine the track's wear rate (optical microscope Contour GT-I, Bruker Nano Surfaces Division, Tucson, AZ, USA). The profilometer instrument is driven by Vision software to assess the wear-track image. The profile of the worn track consists of distinct geometric features.

The wear depth, measured with respect to the sample surface, is the potential parameter describing the wear track volume, followed by the width and the wear track perimeter obtained using the optical profile. To scan the majority of the wear track, four-point measurements were taken on the worn track at 3, 6, 9, and 12 o'clock according to clock orientation. Fig. 3 shows the profilometer measurements at 3 and 12 o'clock orientations [27–30].

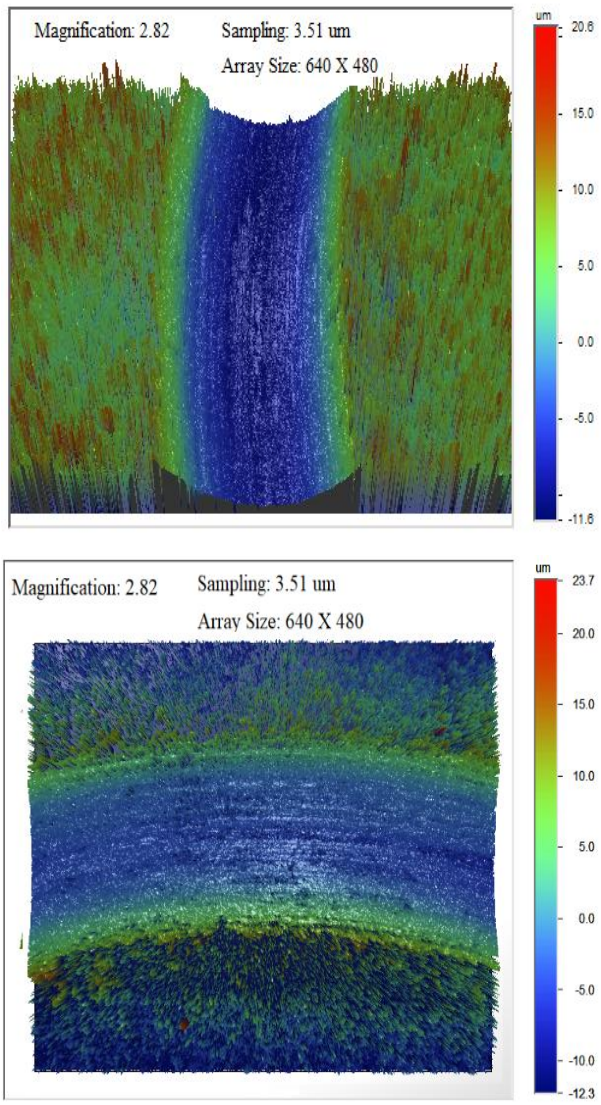

Fig. 3. Profilometer measurements results according to o'clock orientation: (a) 3 o'clock, (b) 12 o'clock

The experimental procedure for measuring the wear volume consists of calculating the elementary section A_i (as illustrated in Fig. 4) for the four sections at 3, 6, 9, and 12 o'clock, which are 90° apart between every two successive sections. A_i is expressed by:

$$A_i = \frac{1}{2}(h_{i+1} - h_i)(w_{i+1} - w_i) \quad (\mu m^2) \qquad (1)$$

where are:

h_i and w_i - are respectively the wear depth and width at i^{th} point of each section of the worn track.

h_{i+1} and w_{i+1} - are respectively the wear depth and width at $(i+1)^{th}$ point of each section of the worn track.

The wear area of each section of the worn track, according to the clock orientation, is expressed by equation (2), and the corresponding wear volume is expressed by equation (3). The mean wear volume of the four sections in the worn track is expressed by equation (4).

$$A_n = \sum_{i=1}^{N-1} A_i \quad (\mu m^2) \qquad (2)$$

$$V_i = 2\pi r A_n \quad (\mu m^3) \qquad (3)$$

$$V = \frac{1}{4}\sum_{n=1}^{4} 2\pi r A_n \quad (\mu m^3) \qquad (4)$$

$$K_i = \frac{V_i}{FD} \quad (\mu m^3/N/m) \qquad (5)$$

where are:

A_n - The total measurement of four elementary wear sections (µm²), Fig.2.

A_i - The measurement of the elementary wear section profile sections 3, 6, 9, and 12 o'clock that are 90° apart between every two successive sections (µm²).

r - Represents the radius of the wear track, calculated as the average of the four measured sections of the worn track (mm) r=5mm.

V_i - The measurement of the elementary wear volume profile sections 3, 6, 9, and 12 o'clock that are 90° apart between every two successive sections(µm³).

V - The total measurement of the wear volume of four elementary wear sections (µm³), Table 7.

F - Applied load P=20 N.

D - Distance traveled D=5000 m.

K_i -Wear rate (µm³/N/m), Table 7.

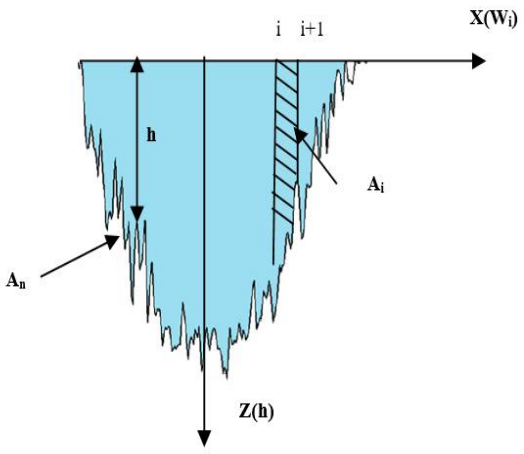

Fig. 4. Elementary wear section profile of the worn track

The coefficient of friction µ is defined as the ratio of the maximum measured friction force amplitude during one cycle to the applied normal load F, as expressed by equation (6).

$$\mu_i = \frac{f_i}{F} \qquad (6)$$

where are:

μ_i and f_i - represent the friction coefficient and the friction force at the i^{th} increment, respectively.

3. RESULTS AND DISCUSSION

3.1. Friction Coefficient

It is noteworthy that the ball travels 500 mm each second. Hence, with eight laps (track distance) equaling one cycle in one-half second, the ball will traverse two cycles per second. Fig. 5 depicts the experimental results of the 2 hours 46 minutes long-term dry friction test as a function of the cycle number, a sliding speed of 0.5 m/s, and applied force (20 N). These values have been set appropriately for this type of Tungsten carbide-based material with a fraction of Titanium carbide and superior tribological performance. Fig. 1 depicts the testing of a material on a high-temperature tribometer using an alumina ball. The outcomes of the friction tests indicate that the coefficient of friction remains stable throughout the test, with an average value of 0.43. Its progression also demonstrates the material's remarkable thermal stability, confirming its excellent tribological performance.

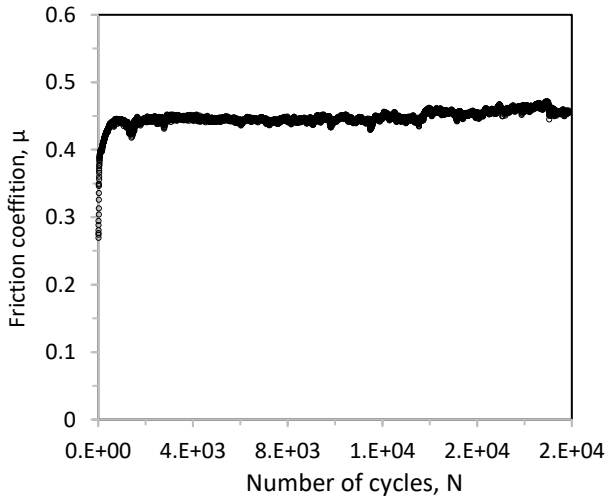

Fig. 5. Evolution of the friction coefficient as a function of the cycle number

The incorporation of 10% TiC into the WC/Co base cermet significantly enhanced the stability of the coefficient of friction, thereby improving the overall tribological performance and extending the service lifetime of the material. This improvement is primarily attributed to the excellent thermomechanical properties of TiC, including its very high hardness 2800–3200 HV, high melting point approximately 3067–3160°C, superior thermal stability up to 800°C under oxidizing conditions, and high mechanical strength resulting from its strong covalent bonding.

3.2. Statistical Analysis of the Friction Coefficient

The main objective of this analysis is to determine whether the coefficient of friction (COF) remains stable during the friction test at 650°C. Furthermore, the probability density function and cumulative distribution function must be established to verify whether the friction behavior is predictable and falls within acceptable limits with a high level of confidence. Finally, the statistical analysis aims to distinguish the different phases of the test: identifying and analyzing specific time intervals, such as the break-in period and steady-state phases, to ensure the reliability of the measured quantity during different tests [34].

3.2.1 Including Break-in Period

As shown in Figure 5, the coefficient of friction of the developed cermet stabilizes after approximately 1075 cycles during the disc wear test. That stabilization marks the end of the initial break-in period, indicating the formation of a stable, reproducible friction regime. Such behavior reflects well-defined contact conditions and a consistent wear mechanism, which allows for a reliable long-term tribological performance evaluation of the cermet. Consequently, the stable frictional response enhances the material's suitability for practical applications and provides valuable guidance for material selection in various industrial sectors.

In addition, the 1075 cycles of the break-in phase can be important for understanding the cermet's adaptability during the early cycles, and the analysis can provide insights into how the material behaves during the initial stages of wear.

A statistical analysis was performed to reveal the probability density function of the friction coefficient to understand how the materials behave. Additionally, this information can be valuable for modelling, predicting, optimizing materials and processes, and analyzing failures in the field of tribology. Additionally, describing the probability density of the friction coefficient using a mathematical function is required for data analysis.

As a usual choice, the normal density function, as illustrated in Fig. 6 and Fig. 7 with a dashed line, might overlook how the cermet actually handles friction. However, modelling the friction coefficient with the logistical density law shows the unique details of the pin-on-disc test in a more realistic way. Besides, the experimental data of the tribological

behavior of the developed cermet in pin-on-disc, picking the normal distribution law, makes the assessment overlook the real details of how this cermet handles friction. On the contrary, modelling the friction coefficient of the developed cermet with the logistic law appears closer to the experimental data. The corresponding parameters of the normal and logistic law are illustrated in Table 5. This latter summarizes the comparison between the two distributions for the friction test. For instance, the log-likelihood for the logistic distribution (32905) is higher than that for the normal distribution (31037), indicating a better fit to the data for the logistic probability density function. In addition, the logistic distribution has a narrower spread than the normal distribution, and covariance analysis shows that its parameters are less correlated than those of the Gaussian distribution. Furthermore, the analysis of the cumulative distribution function was conducted to better understand the characteristics of the distribution. Equations (7) and (8) present the mathematical expressions of the Logistic probability density function and cumulative density function of the cermet friction coefficient.

Probability density function:

$$f(x) = \frac{\pi}{\sigma\sqrt{3}} \frac{exp\left[-\frac{\pi}{\sigma\sqrt{3}}(x-m)\right]}{\left[1+exp\left[-\frac{\pi}{\sigma\sqrt{3}}(x-m)\right]\right]^2} \quad (7)$$

where are:

σ - Standard deviation,

m - Mean value.

Cumulative density function:

$$F(x) = \frac{1}{1+exp\left[-\frac{\pi}{\sigma\sqrt{3}}(x-m)\right]} \quad (8)$$

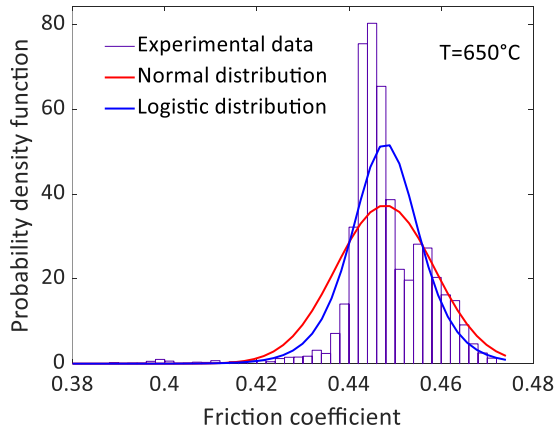

Fig. 6. Probability density function of the friction coefficient parameter

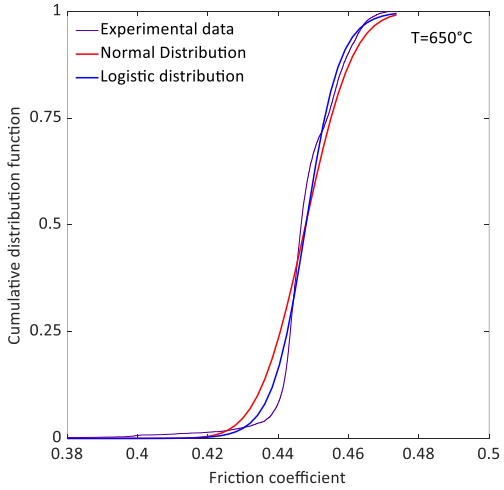

Fig. 7. Cumulative distribution function of the friction coefficient parameter

Table 5. Statistical analysis for the friction coefficient test

Parameter	Normal distribution	Logistic distribution
Log-Likelihood	31037	32907
Mean (μ)	0.448	0.448
Standard Deviation (σ)	0.0107	0.00480
Covariance (μ)	1.14×10^{-8}	6.74×10^{-9}
Covariance (σ)	2.84×10^{-21}	$2.091.14\times10^{-10}$

3.2.2 Removing Break-in Phase

In this section, the break-in period is excluded from the data analysis in order to investigate the steady-state behavior of the cermet after stabilization. This can help focus the analysis on the more consistent and predictable behavior of the developed cermet. Fig. 8 shows the evolution of the friction coefficient as a function of cycle number (without a break-in period).

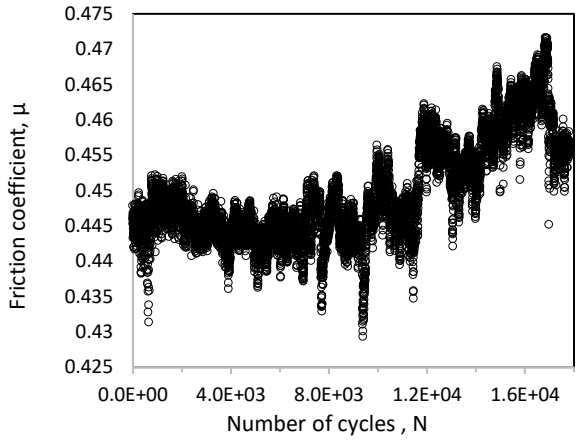

Fig. 8. Evolution of the friction coefficient as a function of the cycle number (without break-in period)

A statistical analysis has been performed to determine the best distribution fit for the friction coefficient. The experimental data of the friction coefficient have been fitted using normal, logistic, and extreme value distributions as illustrated in Fig. 9. It is obvious that the extreme value distribution has been identified as the best fit, and appears to be the most suitable model for describing the friction coefficient in the pin-ion disc system.

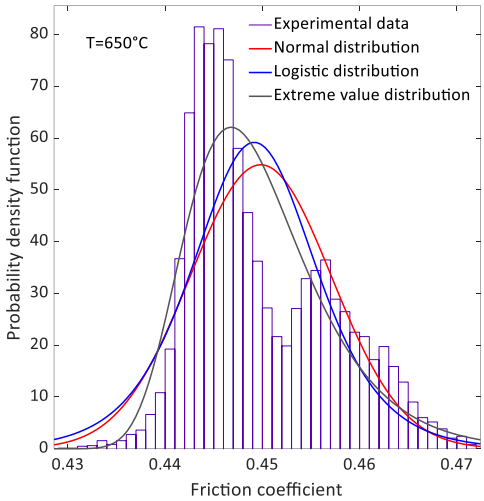

Fig. 9. Probability density function of the friction coefficient parameter (without break-in period)

Table 6 summarizes the comparison between the three distributions for the friction test.

Table 6. Statistical analysis of the friction coefficient test (without break-in period)

Parameter	Normal distribution	Logistic distribution	Extreme value distribution
Log-Likelihood	31266	31143	31143
Mean (μ)	0.449	0.449	0.449
Standard Deviation (σ)	0.00714	0.00410	0.00576
Covariance (μ)	5.75×10^{-9}	5.88×10^{-9}	6.16×10^{-5}
Covariance (σ)	7.78×10^{-22}	2.82×10^{-10}	1.149×10^{-7}

3.3. Wear Volume

Fig. 10 shows four wear profiles of a single worn track, oriented as in Fig. 2a, as recorded by a 2D profilometer (width and depth). The elementary wear section profile of the worn track, as illustrated in Fig. 4, along with the wear surface, wear volume, and wear rate at the four measurement points on the worn track (Table 7), are assessed using Eq. (2–5).

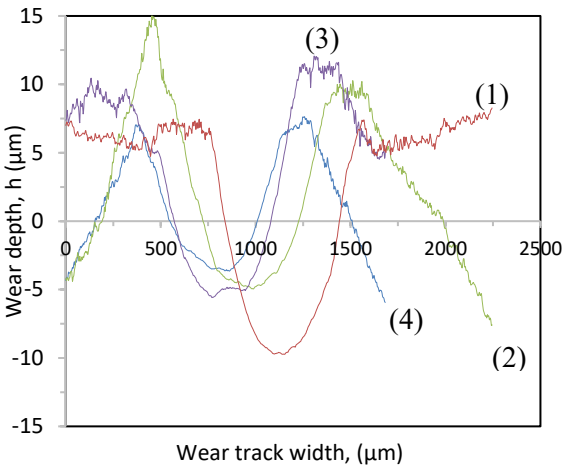

Fig. 10. Wear profile through the wear track width

Table 7. Volume and wear rate measurement of the four profiles of a worn track

Measurement point	Total surface, A_i (μm²)	Wear volume, V_i (μm³)	Wear rate, K_i (μm³/N/m)
1	1755	55×10^6	551
2	1784	56×10^6	560
3	994	31×10^6	312
4	1121	35×10^6	352

The Wear rate of the investigated cermet, based on the elementary wear section profile, shows that measurement points (1) and (2) have the highest wear rate estimated between 551 and 560 μm³/Nm, while points (3) and (4) exhibit the lowest wear rate, ranging from 312 to 352 μm³/Nm. In addition, a variation of 40% in the wear rate between the four points was noted, attributed to the Hertzian contact pressure between the sample (cermet) and the alumina ball. This variation is also attributed to the heterogeneity in the distribution of 10% TiC and the arbitrary selection of measurement points of the worn track. The first note in the comparison of the four profiles of a worn track reveals a significant difference in wear volume, ranging from 3.1×10-2 to 5.6×10^{-2} mm³. For the wear rate, if we take the lowest value as a reference, the error of calculation in the four profiles of a worn track are 76%, 79%, and about 13% in the measurement points (1), (2), and (4), respectively. The average wear rate of the worn track is estimated to be 449 (μm³/Nm), which is represented by the horizontal straight line in Fig. 11. It should be noted that the Archard equation and hence the wear rate should be based solely on adhesive wear. It is well known that adhesive wear is the primary wear mechanism of the developed cermet. The Archard wear equation (9) represents the wear rate as the ratio of the wear volume to the

product of the normal contact load and the sliding distance. Fig. 11 shows the results of the wear rate according to the Archard model based on the experimental volume assessment using the above-developed methodology.

$$K = V/FS \quad (9)$$

where are:
V - wear volume of four (µm^3**),**
F - Applied load (N),
S - sliding distance (m),
K - Wear rate (µm³/N/m).

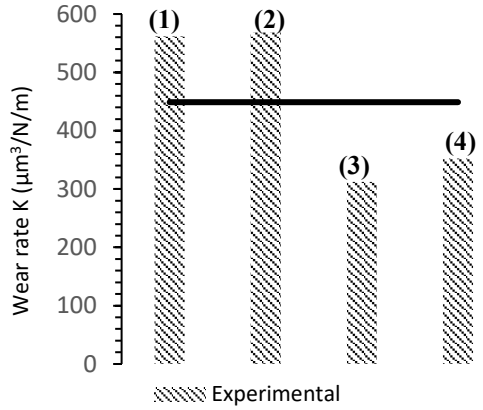

Fig. 11. Wear rate of the developed cermet

3.4. Microstructural Analysis

The SEM Analysis of the microstructure of the worn cermet track (Tungsten carbide and Titanium) is performed to identify the dominant wear mechanisms. Collected debris particles generated from WC-Co-10%TiC cermet are irregular in shape with sharp edges, as shown in Fig. 12 (b,c). The average size of the wear debris ranges from 0.1 to 0.25 µm for the investigated cermets. During sliding wear, initial Hertzian contact pressure deforms the binder phase composed of Co, while the applied load is carried by the harder ceramic grains (TiC, WC). The SEM image also shows formation of a core-rim morphology, which is suggested to result from dissolution and reprecipitation during the sintering process. For the cermet WC-Co-10%TiC, it is observed that the structure was more uniform without any appreciable appearance of porosity or oxides. Additionally, the cohesion is superior due to the interlocking of carbides within the cobalt matrix. This analysis reveals a track formed by oxidized debris, which explains the influence of test parameters and the generation of an oxidized layer. The worn surface of the cermet against an alumina ball reveals the presence of grain tearing, adhesion, and the formation of layers of morphology (in the form of a plate). In addition, this layer is likely to be the result of successive adhesion and transfer of debris (Fig. 12a). Also, the SEM analyses revealed that the cermet was composed of tungsten carbide and microcracks, as illustrated in (Fig. 12. b,c).

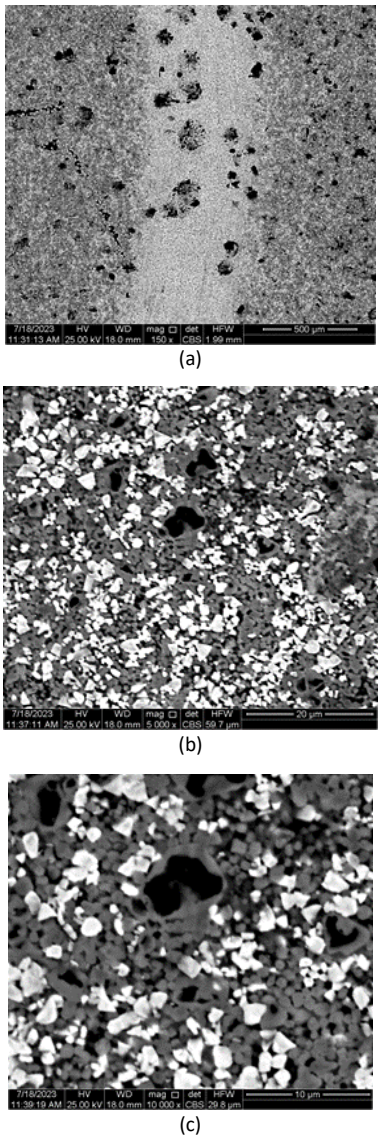
(a)
(b)
(c)

Fig. 12. SEM images of the wear tracks on the cermet

The SEM/EDS analyses at points (P1), (P2), and (P3), Fig. 13, show spectra with different peaks corresponding to elements (C, O, Ti, Co, W) arising from the alumina Al_2O_3 and the cermet (WC, Co, TiC) under the parameters F=20 N, V=0.5 m/s, and 650°C. EDS analysis of wear debris reveals the presence of Ti, W, C, Co, and O, corresponding to the cermet composition. The SEM/EDS images of all cermets reveal three major phases: (W), (Ti), and (Co). The analysis further suggests that the black core phase corresponds to (Ti), while the gray rim phase is a solid solution of (Ti, W, Co). This analysis indicates that wear is primarily generated by oxidized debris, leading to the formation of an oxide

rich in tungsten (W) at points (P1), (P2), and (P3). This is confirmed by the spectra analysis of different elements, as illustrated in Table 8. This oxidized zone generated in the wear track promotes the creation of resistance to wear, which is confirmed by the value and stability of the obtained coefficient of friction. This analysis also confirms that oxygen forms a major chemical component within the tribolayer arising from the cermet and alumina ball. This very compact oxidized layer (tribofilm) distributed over the entire wear track, rich in (W) at the different points (P1), (P2), and(P3), as well as the presence of the different elements of the material (Ti, C, Co), confirms the homogeneity across the entire track. In addition, the spectra on the wear traces prove that there is a material transfer process from the alumina ball, indicating a wear transfer mechanism between the ball and the material at the different points.

Table 8. Different elements of the spectra (P1, P2, and P3) SEM/EDS at different points of the used track

Elements	Spectrum (P1)	Spectrum (P2)	Spectrum (P3)
C	16.34	12.27	15.69
O	15.08	4.24	19.47
Ti	15.49	0	10.75
Co	4.21	4.16	7.97
W	48.89	78.62	46.12

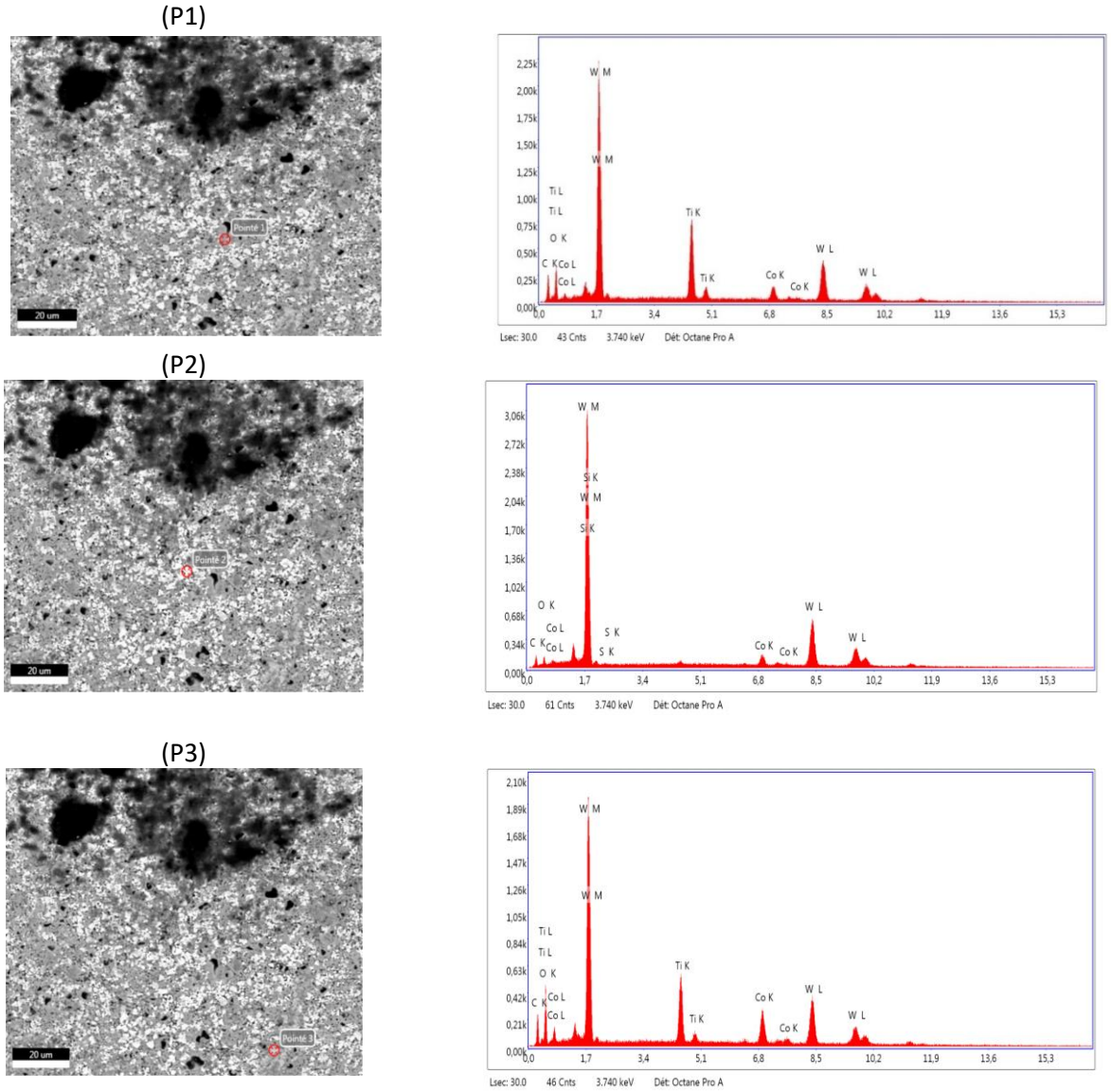

Fig. 13. SEM/EDS analyzes at points (P1), (P2) and (P3) of titanium carbide (WC-Co-10%TiC) at the parameter

4. CONCLUSION

The present investigation focuses on the tribological behavior of a cermet elaborated by powder metallurgy, and made mostly of tungsten carbide, cobalt, and titanium carbide. Extensive experimental work in the pin-on-disc test has been carried out in order to assess the tribological behavior of the developed material. The typical hardness HRC and density of the elaborated material are 74.4 N/mm^2 and 11.74 g/cm^3, respectively. The obtained wear track appeared after 2 hours and 46 minutes (5000 m) of sliding distance, and was analyzed using a 3D optical profilometer. The material (cermet) has exhibited excellent stability, which confirms its excellent tribological performance. The main conclusions are summarized below:

- The developed material (cermet) exhibits a perfect stability of the friction coefficient μ=0.43, and a remarkable thermal stability confirming its excellent tribological performance.
- The steady state coefficient of friction varies from 0.27 to 0.47, and the wear rate changes from 312 to 551 μm^3/Nm.
- The friction coefficient of the developed cermet stabilizes after 1075 cycles which can provide insights into how the material behaves during the initial stages of wear.
- The logistic distribution of the friction coefficient has a narrower spread compared to the normal distribution, and the covariance analysis has shown that the parameters in the logistic distribution are less correlated compared to the Gaussian one.
- Without a break-in period, the extreme value distribution has been identified as the best fit, and appears to be the most suitable model for describing the friction coefficient.
- The comparison of the four profiles of a worn track shows a significant difference in wear volume between 3.1×10^{-2} and 5.6×10^{-2} mm^3 indicates heterogeneity in the distribution of TiC 10% and the choice of measurement points.
- The SEM/EDS analysis of the microstructure of the worn cermet track shows that an oxidized zone was generated in the wear track, which promises a high resistance to wear. This is confirmed by tribolayer formation and stability of the obtained friction coefficient.
- The microstructure indicates a very compact oxidized layer (tribofilm) distributed over the entire wear track, rich in tungsten (W) at different points (P1, P2, P3), as well as the presence of various elements of the material (Ti, C, Co) in different percentages.
- The results showed that the variation in the coefficient of friction and the wear rate between repeated tests was not statistically significant, thus confirming the reliability and reproducibility of the tribological behavior of the cermet material.
- The correlation analysis also showed that the wear rate is more responsive to normal load than to sliding speed within the tested range.
- The presented results provide a good baseline for predicting the long-term performance in the practical application of this material.
- The results of this study have significant implications for industries using high-performance cermets, including cutting and machining tools, aerospace components, hot rolling dies, and other high-load machines.

CONFLICT OF INTEREST

The authors declare no conflict of interest.

REFERENCES

[1] Z. Sun, X. Zhang, X. Li, Z. Xu, C. Li, Z. Wang, Study on the wear behavior of $CoCrFeNiAl_{1.0}$ high entropy alloy at high temperature. *Materials Letters*, 324, 2022: 132726. https://doi.org/10.1016/j.matlet.2022.132726

[2] Y. Yang, C. Zhang, D. Wang, L. Nie, D. Wellmann, Y. Tian, Additive manufacturing of WC-Co hardmetals: a review. *The International Journal of Advanced Manufacturing Technology*, 108(5) 2020: 16531673. https://doi.org/10.1007/s00170-020-05389-5

[3] R. Harouz, A. Lakehal, K. Khelil, O. Dedry, S.N. Hashemi, S. Boudebane, Dry sliding friction and wear of the WC/TiC-Co in contact with AL_2O_3 for two sliding speeds. *Facta Universitatis. Series, Mechanical Engineering*, 20(1), 2022: 37-52. https://doi.org/10.22190/FUME200310039H

[4] H.C. Liu, B.B. Zhang, N. Bader, G. Poll, C.H. Venner, Influences of solid and lubricant thermal conductivity on traction in an EHL circular contact. *Tribology International*, 146, 2020: 106059.

https://doi.org/10.1016/j.triboint.2019.106059

[5] M. Górnik, E. Jonda, L. Łatka, M. Nowakowska, M. Godzierz, Influence of spray distance on mechanical and tribological properties of HVOF sprayed WC-Co-Cr coatings. *Materials Science-Poland,* 39(4), 2021:545-554. https://doi.org/10.2478/msp-2021-0047

[6] K. Bonnya, P. De Baetsa, Y. Pereza, J. Vleugelsb, B. Lauwers, Friction and wear characteristics of WC-Co cemented carbides in dry reciprocating sliding contact. *Wear*, 268(11-12) 2010: 1504–1517. https://doi.org/10.1016/j.wear.2010.02.029

[7] Q. Su, S. Zhu, H. Ding, Y. Bai, P. Di, Effect of the additive VC on tribological properties of WC-Al_2O_3, composites. *International Journal of Refractory Metals and Hard Materials,* 75. 2018: 111–117. https://doi.org/10.1016/j.ijrmhm.2018.04.005

[8] R. Harouz, A. Lakehal, K. Khelil, Machine learning application for wear rate prediction of WC/Co-based cermet with different content of Ni, Cr, TiC, TaC, and NbC. The International *Journal of Advanced Manufacturing Technology*, 135(11), 2024: 5945-5959. https://doi.org/10.1007/s00170-024-14862-4

[9] L. Espinosa, V. Bonache, M.D. Salvador, Friction and wear behaviour of WC-Co-Cr_3C_2-VC cemented carbides obtained from nano-crystalline mixtures. *Wear*, 272, 2011: 62–68. https://doi.org/10.1016/j.wear.2011.07.012

[10] T. Kagnaya, C. Boher, L. Lambert, M. Lazard, T. Cutard, Wear mechanisms of WC–Co cutting tools from high-speed tribological tests. *Wear*, 267(5-8),2009: 890-897. https://doi.org/10.1016/j.wear.2008.12.035

[11] M. Mottaghi, M. Ahmadian, Sliding wear behavior of the WC/FeAl-B intermetallic matrix composites at high temperatures. *Boletín de la Sociedad Española de Cerámica y Vidrio*, 60(6), 2021: 347–357. https://doi.org/10.1016/j.bsecv.2020.03.010

[12] D. Jianxin, Z. Hui, W. Ze, L. Yansong, Z. Jun, Friction and wear behaviors of WC/Co cemented carbide tool materials with different WC grain sizes at temperatures up to 600◦C. *International Journal of Refractory Metals and Hard Materials*, 31, 2012: 196–204. https://doi.org/10.1016/j.ijrmhm.2011.11.003

[13] F.E. Kennedy, Y. Lu, I. Baker, Contact temperatures and their influence on wear during pin-on-disk tribo testing. *Tribology International*, 82, 2015: 534-542. https://doi.org/10.1016/j.triboint.2013.10.022

[14] V. Gavrish, T. Chayka, G. Baranov, A.Y. Oleynik, Y.O. Shagova, Investigation of the influence of tungsten carbide nanopowder WC and the mixture of tungsten carbides and titanium carbides (WC, TiC) on the change of concrete performance properties. *Journal of Physics, Conference Series*, 1866, 2021: 012008. https://doi.org/10.1088/1742-6596/1866/1/012008

[15] M.A. Alipovna, K.A. Karaulovich, P.A. Vladimirovich, A.Z. Zhanuzakovich, K.B. Bolatovna, W. Wieleba, T. Leśniewski, N. Bakhytuly, The study of the tribological properties under high contact pressure conditions of TiN, TiC and TiCN coatings deposited by the magnetron sputtering method on the AISI 304 stainless steel substrate. *Materials Science-Poland*, 41(1), 2023: 1-14. https://doi.org/10.2478/msp-2022-0055

[16] C. Saravanan, K. Subramanian, V. Anandakrishnan, S. Sathish, Tribological behavior of AA7075-TiC composites by powder metallurgy. *Industrial Lubrication and Tribology*, 70(6), 2018: 1066-1071. https://doi.org/10.1108/ILT-10-2017-0312

[17] F. Toptan, A. Kilicarslan, A. Karaaslan, M. Cigdem, I. Kerti, Processing and microstructural characterisation of AA 1070 and AA 6063 matrix B_4C_p reinforced composites. *Materials & Design*, 31, 2010: 8791. https://doi.org/10.1016/j.matdes.2009.11.064

[18] J. Zheng, K. Lu, Electrically conductive and thermally stable SiC-TiC containing nano composites via flash pyrolysis. *Journal of the American Ceramic Society*, 104(6), 2021: 2460-2471. https://doi.org/10.1111/jace.17663

[19] H. Asgharzadeh, M. Sedigh, Synthesis and mechanical properties of Al matrix composites reinforced with few-layer graphene and graphene oxide. *Journal of Alloys and Compounds*, 728, 2017: 47-62. https://doi.org/10.1016/j.jallcom.2017.08.268

[20] S.A. Alidokht, P. Manimunda, P. Vo, S. Yue, R.R. Chromik, Cold spray deposition of a Ni-WC composite coating and its dry sliding wear behavior. *Surface and Coatings Technology*, 308, 2016: 424-434. https://doi.org/10.1016/j.surfcoat.2016.09.089

[21] R. Harouz, S. Boudebane, A. Lakehal, O. Derdy, H.-M. Montrieux, Investigation of the tribological behaviour of WC/TiC based cermets in contact with Al2O3 alumina under high temperature. *Journal of the Mechanical Behavior of Materials*, 27(1-2), 2018: 1-11. https://doi.org/10.1515/jmbm-2018-0004

[22] M. Sribalaji, B. Mukherjee, A. Islam, A.K. Keshri, Microstructure and mechanical properties of (Ti, W) C–Ni cermet prepared using a nano-sized TiC–WC powder mixture. *Journal of Alloys and Compounds*, 639, 2015: 21-26. https://doi.org/10.1016/j.jallcom.2015.03.115

[23] Y.F. Liu, Z.C. Feng, F. Pu, Z.Y. Xia, G.B. Sun, L.H. Zhang, C.X. Shi, Z. Zhang, Microstructure and dry-sliding wear properties of TiC/CaF2/ γ -Ni self-lubricating wear-resistant composite coating produced by co-axial powder feeding plasma transferred arc (PTA) cladding process. *Surface and Coatings Technology*, 345, 2018: 61-69. https://doi.org/10.1016/j.surfcoat.2018.04.003

[24] X.H. Gao, Z.M. Guo, Q.F. Geng, P.J. Ma, A.Q. Wang, G. Liu, Microstructure, chromaticity and thermal stability of SS/TiC-WC/$A_{l2}O_3$ spectrally selective solar absorbers. *Solar Energy Materials and Solar Cells*, 164, 2017: 63-69. https://doi.org/10.1016/j.solmat.2017.02.009

[25] S. Sten, J. Odqvist, S. Norgren, P. Hedström, Development of a functional hardness gradient in WC-TiC-Co cemented carbide during gradient sintering. *International Journal of Refractory Metals and Hard Materials*, 115, 2023: 106293. https://doi.org/10.1016/j.ijrmhm.2023.106293

[26] C. Jin, C.C. Onuoha, Z.N. Farhat, G.J. Kipouros, K.P. Plucknett, Reciprocating wear behaviour of TiC-stainless steel cermets. *Tribology International*, 105, 2017: 250–263. https://doi.org/10.1016/j.triboint.2016.10.012

[27] A.K. Basak, J.P. Celis, M. Vardavoulias, Abrasive wear of nanostructured cermet coatings in dry and slurry conditions. *International Journal of Refractory Metals and Hard Materials*, 100, 2021: 105638. https://doi.org/10.1016/j.ijrmhm.2021.105638

[28] R.K. Moharana, T. Dash, T.K. Rout, Preparation of Iron Bonded Tungsten Carbide–Titanium Carbide Composites with Improved Microstructure for Designing Various Harder Components. *Journal of Materials Engineering and Performance*, 33(11), 2024: 5479–5486. https://doi.org/10.1007/s11665-024-09341-6

[29] N. Hashemi, A. Mertens, H.M. Montrieux, J.T. Tchuindjang, O. Dedry, R. Carrus, J. Lecomte-Beckers, Oxidative wear behaviour of laser clad high speed steel thick deposits: Influence of sliding speed, carbide type and morphology. *Surface and Coatings Technology*, 315, 2017:519-529. https://doi.org/10.1016/j.surfcoat.2017.02.071

[30] J.C.G. Milan, M.A. Carvalho, R.R. Xavier, S.D. Franco, J.D.B. De Mello, Effect of temperature, normal load and pre-oxidation on the sliding wear of multi-component ferrous alloys. *Wear*, 259(1-6), 2005: 412–423. https://doi.org/10.1016/j.wear.2005.02.050

[31] M. Pellizzari, D. Cescato, M.G. De Flora, Hot friction and wear behaviour of high speed steel and high chromium iron for rolls. *Wear*, 267(1-4), 2009: 467–475. https://doi.org/10.1016/j.wear.2009.01.049

[32] N.G.S. Kumar, T.R. Prabhu, R.K. Mishra, N. Eswaraprasad, G.S.S. Shankar, S. Basavarajappa, Analysis of dry sliding wear behavior of the nano composites using statistical methods with an emphasis on temperature effects. *Measurement*, 128, 2018: 362-376. https://doi.org/10.1016/j.measurement.2018.06.064

[33] F. Hakami, A. Pramanik, N. Islam, A. Basak, N. Ridgway, Study of effective parameters on wear behavior of rubbers based on statistical methods. *Polymers for Advanced Technologies,* 30(6), 2019: 1415-1426. https://doi.org/10.1002/pat.4574

[34] F.O. Kolawole, S.K. Kolawole, Statistical model for predicting friction coefficient and wear of duplex CrN/DLC and nano-multilayer DLC-W coatings using ANOVA. *Discover Materials*, 4, 2024: 36. https://doi.org/10.1007/s43939-024-00099-1